Alexandria Engineering Journal (2016) 55, 619–625

HOSTED BY

ELSEVIER

Alexandria University

Alexandria Engineering Journal

www.elsevier.com/locate/aej
www.sciencedirect.com

ORIGINAL ARTICLE

Facile synthesis of zero valent iron magnetic biochar composites for Pb(II) removal from the aqueous medium

M. Rama Chandraiah *

JNTUA College of Engineering, Department of Chemistry, Kalikiri, Chittoor 517237, AP, India

Received 25 May 2015; revised 17 October 2015; accepted 20 December 2015
Available online 12 February 2016

KEYWORDS

E. globules bark;
ZVI-MBC;
FT-IR;
TEM;
Adsorption of Pb(II)

Abstract New zero valent iron magnetic biochar composites (ZVI-MBC) were synthesized by facile method using *Eucalyptus globules* bark waste. The as-prepared ZVI-MBC was used as an adsorbent for the removal of Pb(II) from aqueous solution. Fourier transform infrared spectroscopy (FT-IR), X-ray diffraction (XRD), transmission electron microscopy (TEM) and energy-dispersive spectroscopy (EDS) were used for characterization of ZVI-MBC. Effect of variable parameters including pH, contact time and initial concentration of metal ions was studied. The ZVI-MBC exhibited good adsorption performance over the initial pH at 6. The adsorption isotherm data were fitted well to Langmuir isotherm then Freundlich model, and the adsorption capacity was found to be 60.8 mg/g at 303 K. The kinetic data were studied by applying two adsorption kinetic models, pseudo-first- and pseudo-second-order equations. The experimental kinetic data fitted very well to the pseudo-second-order model. The experimental results herein suggest that ZVI-MBC can be used as low cost-effective material for the removal of Pb(II) from water systems with a simple magnetic separation process.

1. Introduction

Due to the rapid development of industrial and agricultural production processes, contamination by toxic heavy metal ions in aqueous systems generates great concern for the natural environment and human health [16] Lead (Pb(II)) is commonly present in effluents due to its wide application in many industrial processes such as mining, refineries, painting, metal plating and cleaning, battery and car radiator manufacturing and agricultural activities [22,19]. Lead is highly toxic and can cause a variety of negative effects on human health such as lead is linked to reproductive and nervous system problems, high blood pressure, kidney damage, memory and concentration difficulties and, in high amounts, coma, convulsions and death [20]. The permissible limit of lead in drinking water as set by the World Health Organization is 10 μg/L [26]. Therefore there have been many efforts to reduce the concentration of lead ions in effluent wastewater [21]. In this concern, to eliminate metal pollutants from aqueous solutions a wide

* Tel.: +91 9441123509.
E-mail address: drrcrjntuacek@gmail.com.
Peer review under responsibility of Faculty of Engineering, Alexandria University.

http://dx.doi.org/10.1016/j.aej.2015.12.015

variety of techniques including chemical precipitation, evaporation, ion-exchange, adsorption, cementation, electrolysis, and reverse osmosis have been developed [2]. Among these existing methods, adsorption has become one of the most promising and effective techniques due to its better performance, availability of different adsorbents, easy operation, and low cost. Therefore, much attention has been paid to developing inexpensive, practical sorbents with potential applications in metal removal from aqueous solutions [14]. However, to overcome these limitations, an inexpensive and environmentally eco-friendly adsorbent with high removal efficiency for lead is needed. Thus extensive research has been focused on the utilization of biomass residues which are abundantly available throughout the world for this purpose. Biochar is a carbon rich, solid by-product resulting from the pyrolysis of biomass under oxygen-free and low temperature conditions [1]. Biochar has a large specific surface area, microporous structure, active functional groups, and high pH, which may be good for its use as a surface sorbent [6,8,9]. Adsorbents in the form of biochars produced from agricultural waste or by-products may be inexpensive sorbents for the removal of Pb(II) [4]. However, powdered biochar, such as powdered active carbon, was difficult to be separated from the aqueous solution. Magnetic biochar particles can be easily separated from the aqueous solution by using an external magnetic field. In addition, the unique properties of magnetic biochar materials provide many opportunities to overcome current obstacles in adsorption process. Hence, introducing magnetic medium (e.g., magnetite, γ-Fe_2O_3 and ZVI-MBC) to the premade or commercial sorbent (e.g., active carbon and carbon nanotubes) is an efficient method to enable the sorbent to be effectively separated by magnetic separating technique [29,8,9,30,5]. Therefore, in recent years much attention has been paid to develop magnetic biochar composites using biomass residues.

In the literature several biomass materials such as agricultural wastes, wood waste, forestry residues, animal manures and food wastes are used for biochar production [17,3]. In the present study, we have chosen *Eucalyptus globules* (*E. globules*) bark waste which is inexpensive and abundantly available in India and also used as adsorbent for removal of metals [18]. Owing to its abundant availability, economic feasibility and the presence of various functional groups that were useful in producing the magnetic composite, in this study we have chosen *E. globules* bark waste as a precursor for the production of zero valent magnetic biochar composite (ZVI-MBC). The prepared ZVI-MBC was characterized by various analytical techniques such as FT-IR, XRD, TEM and EDS. The adsorption behavior of Pb(II) ions onto ZVI-MBC was studied under different experimental conditions using batch method. The optimum adsorption conditions for their removal of Pb(II), adsorption isotherms and kinetic studies were extensively studied.

2. Experimental

2.1. Materials

All the reagents used in the present study were of analytical grade. The Pb(II) stock solution was prepared by dissolving the prescribed amount of corresponding metal salt in double distilled water. $FeCl_3$ś$6H_2O$ (Ferric hexachloride) was purchased from Sigma–Aldrich. Desired concentration of standard solution was obtained by dilution of stock solution with double distilled water. The pH of the solutions was adjusted by the addition of either 0.1 M HCl or 0.1 M NaOH solution.

2.2. Preparation of ZVI-MBC

E. globules bark waste residues were collected from Tirumala (Chittoor), AP, South India. The collected barks were washed with tap water followed by distilled water to remove dirt and air-dried. Then they were cut into small pieces and were powdered by using mixture grinder. The bark powder was pyrolyzed at 750 °C and the resultant biochar was used for the preparation of the ZVI-MBC. The biochar composite was magnetized by the impregnation of the ZVI on the biochar surface. For magnetization, in a unique reaction procedure, 5.4 g of $FeCl_3$ś$6H_2O$ was dissolved in 100 ml of double distilled water and honey was added dropwise for reduction of Fe^{3+} to Fe^0 then the mixture was stirred vigorously for 30 min. The biochar composite (10 g) was added slowly into the above reaction mixture and stirred vigorously at 1000 rpm for 60 min. After stirring, the obtained black product was washed three times with ethanol and filtered. The obtained products were dried in a vacuum oven at 90 °C for overnight and stored in a stoppered bottle.

2.3. Characterization

FTIR measurements of *E. globules* bark waste residues and prepared sample were made with Thermo Nicolet FTIR – 200 thermo electron corporation. The crystalline structure of synthesized ZVI-MBC was characterized by X-ray diffractometer Seifert 3003 TT with Cu Kα radiation having a wavelength of 1.54 Å. Morphological and size distribution were done with transmission electron microscope (TEM) images, on JEM-2100 with an accelerating voltage of 200 kV system of jeol, and Quantitative elemental analysis of the nanoparticles was carried out with Oxford instruments Inca Penta FET x 3 electron diffraction spectrum (EDS).

2.4. Batch adsorption studies

Batch adsorption experiments were conducted in a thermostat controlled shaker to determine the optimum operational parameters such as initial pH, contact time, and initial metal concentration. Pb(II) stock solution was prepared with different concentrations, and then 2.5 mg of ZVI-MBC adsorbent was added to 25 mL of each Pb(II) ion solution. For all adsorption tests, the initial pH values of the metal solution were adjusted using 0.1 M HCl/NaOH solution. To understand the pH effect (Elico LI 120) the ZVI-MBC dosage was maintained at 0.1 g/L. The solution mixture was ultrasonicated at room temperature for 5 min, transferred to 100 mL Erlenmeyer flask and was shaken in a thermostatic incubator (200 rpm) at 303 K. The concentration of Pb(II) ions was determined using FAAS (Shimadzu AA – 6300). All the adsorption experiments were repeated triplicate. The equilibrium adsorption capacity (qe) of ZVI-MBC and the removal percentage (%Removal) were calculated by using the following equations:

$$q_e = \frac{(C_i - C_e)V}{M} \quad (1)$$

$$\text{Adsorption } (\%) = \frac{(C_i - C_e)}{C_i} \times 100 \quad (2)$$

where q_e (mg/g) is the equilibrium adsorption capacity of Pb (II). C_i and C_e were initial and equilibrium concentrations (mg/L) of Pb(II) respectively, M is the adsorbent dosage (mg), and V is the volume of the solution (L).

3. Results and discussion

3.1. Characterization of ZVI-MBC

The crystalline structure of the ZVI-MBC was determined by using X-ray diffraction (XRD) analysis and the patterns observed are shown in Fig. 1. The XRD patterns of the ZVI-MBC showing three relatively strong reflection peaks in the 2θ region at 42.9°, 49.9° and 73.3° which correspond to crystal planes (1 1 1), (2 0 0) and (2 2 0) can be well indexed to the face centered cubic structure of ZVINPs (JCPDS card no. 65-4150). The XRD patterns observed confirmed the presence of iron in zero valent state.

The FTIR analysis of the *E. globules* bark powder, ZVI-MBC and Pb(II) loaded ZVI-MBC composites was performed by using FTIR spectra and the results are shown in Fig. 2. However, FTIR analysis was used to confirm the modification procedure and to obtain the information on the presence of various functional groups on the surface of materials. Fig. 2(a) represents the *E. globules* bark powder, (b) ZVI-MBC composites and (c) Pb(II) loaded ZVI-MBC composites. The major components of *E. globules* bark consist of organic polymer substances such as cellulose, hemi cellulose, lignin and polyphenolic acids [27]. A broadband around 3480 cm^{-1} can be assigned to the stretching vibration of OH groups of polymeric compounds predominantly due to the presence of cellulose. The peaks at 2920 cm^{-1} and 2850 cm^{-1} are assigned to alkyl CH_2 stretching and band around 1720 cm^{-1} was due to the presence of carboxyl groups (C═O) [24]. Thus from FTIR spectra data it was observed that *E. globules* bark consists of hydroxyl and carboxylate groups. By comparing the IR spectrum of *E. globules* bark with ZVI-MBC, it is observed that several peaks are shifted and few new peaks corresponding to ZVI are also observed. The bands observed around 3420 cm^{-1}, 1122 cm^{-1} and 886 cm^{-1} are assigned to OH, alcohol group and amine groups. Moreover, the band at 525 cm^{-1} was indication of ZVI [15]. In Fig. 2(c) the bands are slightly changed which is due to chelating of Pb(II) metal ions.

In addition to the above characterization, further TEM and EDS were used to analyze the surface morphology and chemical composition of the composite. Fig. 3 shows the ZVI-MBC composite and the particles are nearly spherical with agglomeration. It is due to biochar having cellulose and other biological functional groups. The ZVI (dark part) particles are unevenly distributed on the biochar surface and inside the pores. Moreover, EDS elementary composition analysis confirmed the presence of Fe ions shown in Fig. 4. In addition with these elements, carbon and oxygen which are predominant elements that represent biochar are present in higher amount.

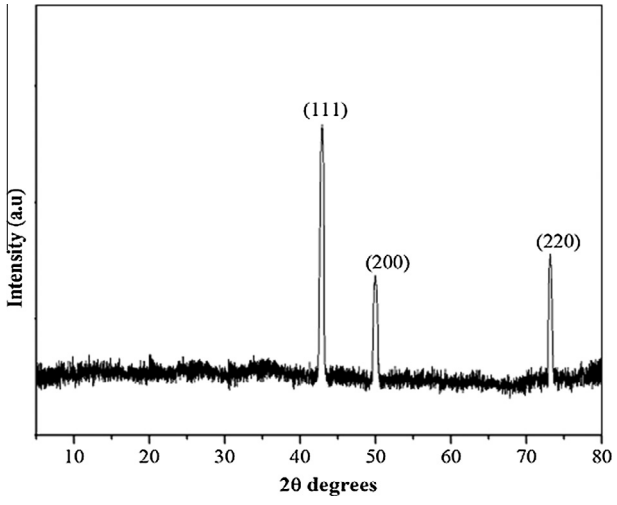

Figure 1 XRD image of ZVI-MBC.

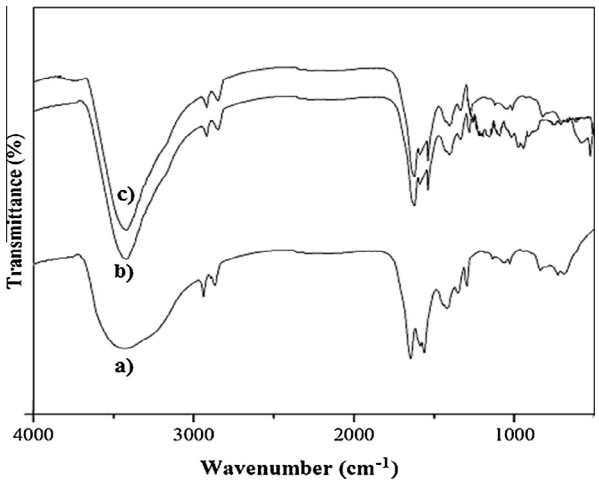

Figure 2 FT-IR spectra of ZVI-MBC.

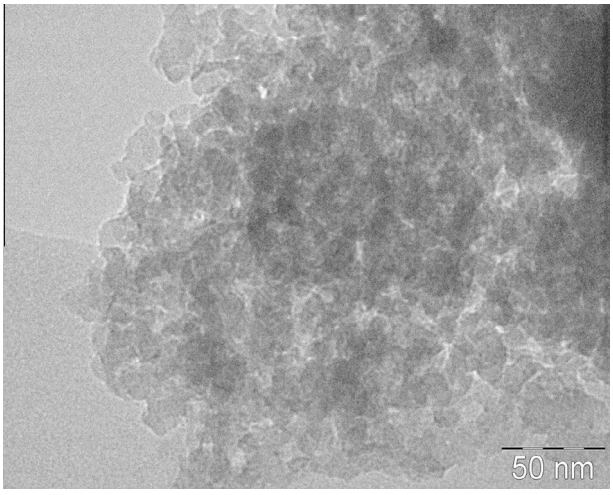

Figure 3 TEM image of facile synthesized ZVI-MBC.

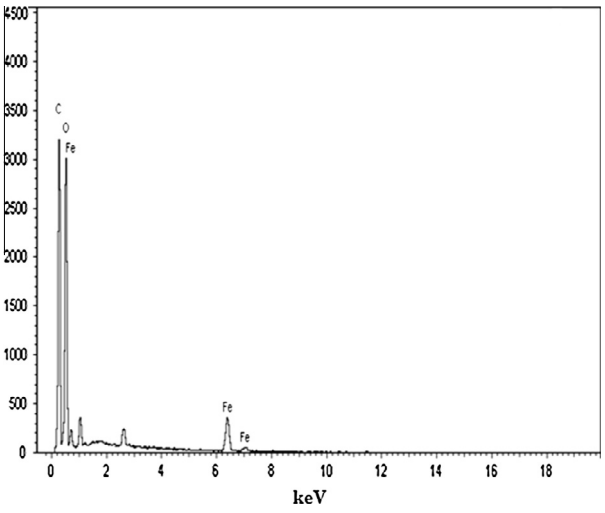

Figure 4 EDX pattern of ZVI-MBC.

3.2. Effect of pH

Batch adsorption process solution pH is one of the important parameters which influences the surface charge and dissociation of functional groups on the adsorbent. Experiments were performed for the removal of Pb(II) ions from the aqueous solution and initial concentrations of 50, 100, 150 and 200 mg/L. As shown in Fig. 5, the percentage removal of Pb (II) increased an increase of pH from 2 to 5 and thereafter removal decreased with an increased pH > 5 and the ZVI-MBC composite displayed a maximum removal of 97.3% at pH 5.0. Less effect was observed when the initial concentration of Pb(II) was 100, 150 and 200 mg/L and the adsorption capacity of ZVI-MBC was below 50%. At low pH, Pb(II) removal was inhibited because the H^+ competed with Pb(II) for adsorption sites. Thus the metal ions cannot move toward the positively charged surface of ZVI-MBC due to electrostatic repulsion and hence a lower removal was observed at low pH values. This significantly affected Pb(II) adsorption at low pH medium. Moreover, at higher pH, electrostatic attraction increases between the adsorbent and metal, which increases adsorption capacity. Decrease in Pb(II) removal at higher pH (pH > 5) is because of the formation of Pb(II) as Pb $(OH)^+$, $Pb(OH)_2^0$, and $Pb(OH)^3$ at different pH values [25]. ZVI-MBC predominantly consists of surface hydroxyl groups (S-OH) which is due to presence of cellulose and surface sites are Lewis-acid type functional groups which are effective for metal ion removal.

3.3. Adsorption kinetic studies

Fig. 6 shows the adsorption behavior of Pb(II) on the ZVI-MBC at initial concentration of 50 mg/L, pH at 5.0 and 303 K as a function of contacting time. The adsorption rate of the Pb(II) on ZVI-MBC was almost finished within 60 min and reached equilibrium. The pseudo-first-order [13,28] and pseudo-second-order [12] kinetic models were used to investigate the removal of kinetics on the ZVI-MBC.

The linear form of pseudo-first-order kinetic model is described by the following equation:

$$\log(q_e - q_t) = \log q_e - \left(\frac{k_1}{2.303}\right)t \tag{3}$$

where k_1 (min^{-1}) is the pseudo-first-order rate constant of adsorption, and q_e (mg/g) and q_t (mg/g) are the amounts of the Pb(II) adsorbed at equilibrium and at time t. The pseudo-first-order kinetic constants were determined from slope of the plot of log $(q_e - q_t)$ vs t. The R^2 value is very less suggesting that the adsorption of Pb(II) ions does not follow pseudo-first-order kinetic model.

The kinetic data were further analyzed using pseudo-second-order kinetic model. The linearized form of the equation is represented as

$$\frac{t}{q_t} = \frac{1}{k_2 q_e^2} + \left(\frac{1}{q_e}\right)t \tag{4}$$

where k_2 (g/mg min^{-1}) is the pseudo-second-order rate constant, and q_e (mg/g) and q_t (mg/g) are the amounts of the Pb(II) adsorbed at equilibrium and at time t. The values of

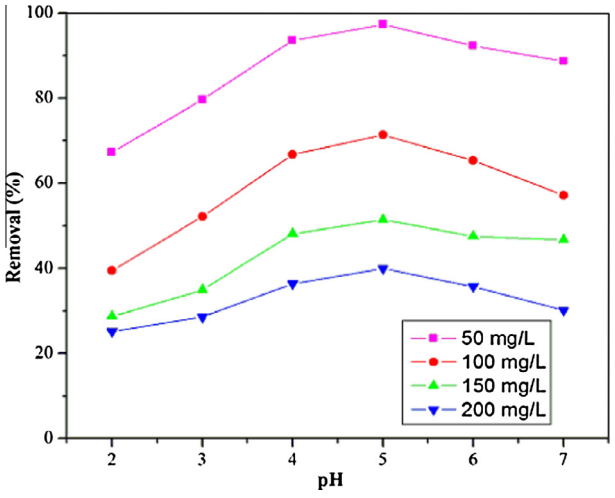

Figure 5 Effect of pH value on the adsorption of Pb(II) by ZVI-MBC at different initial concentrations of Pb(II).

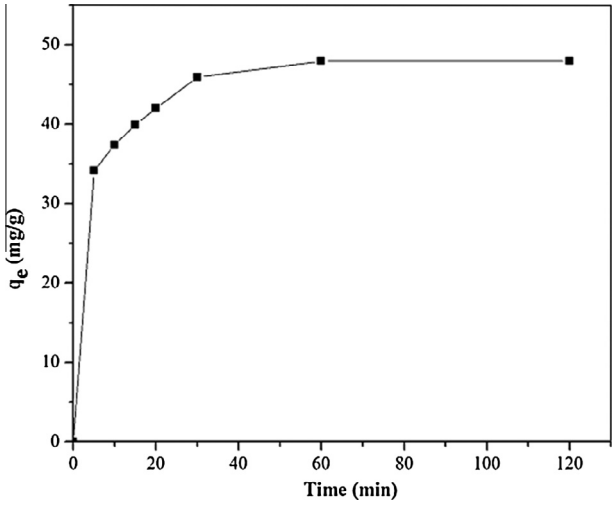

Figure 6 Effect of contact time on the extraction of Pb(II) by ZVI-MBC.

k_2 and q_e can be calculated from the slope and intercept of a plot of t/q_t vs t. From the removal kinetics shown in Fig. 7, the slope shows good linearity with the correlation coefficient value (R^2) which is 0.9998, indicating that the removal kinetic follows the pseudo-second-order model. Table 1 shows the corresponding parameters of the pseudo-second-order model. The adsorption system obeyed the pseudo-second-order kinetic model for the entire adsorption period and thus supported the assumption that the adsorption was the chemisorptions process [7].

3.4. Adsorption isotherm

Langmuir and Freundlich isotherm models revealed the maximum adsorption capacity of adsorbent and the equilibrium adsorption of Pb(II) on ZVI-MBC. The Langmuir equation can be expressed by the linearized form as follows:

$$\frac{C_e}{q_e} = \frac{C_e}{q_m} + \frac{1}{q_m b} \tag{5}$$

where q_e is the equilibrium adsorption capacity of metal on concentration of the adsorbent (mg/g), C_e is the equilibrium metal ion concentration in the solution (mg/L), q_m is the maximum capacity of adsorbent (mg/g), and b (L/mg) is the equilibrium constant relating to the sorption energy. Fig. 8 shows that the experimental data fit the Langmuir adsorption isotherm well, maximum adsorption capacity was found to be 60.8 mg/g as prepared ZVI-MBC at pH = 5.0 and correlation coefficients and equilibrium constants are listed in Table 2. In addition, another parameter in the Langmuir adsorption isotherm, a dimension less factor (R_L) is described by the following equation:

$$R_L = \frac{1}{1 + bC_i} \tag{6}$$

where C_i (mg/g) is initial metal concentration, and b (L/mg) is the Langmuir constant. For favorable sorption, $0 < R_L < 1$; for unfavorable sorption, $R_L > 1$; for irreversible sorption $R_L < 0$; for linear sorption, $R_L < 1$. In this study, the R_L value is 0.0109 which lies between 0 and 1. This indicates that the adsorption of Pb(II) on ZVI-MBC is favorable.

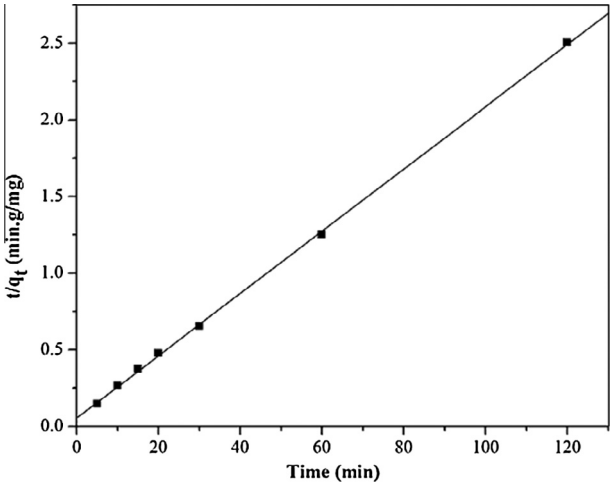

Figure 7 Pseudo second-order adsorption kinetics of Pb(II) on ZVI-MBC.

Table 1 Kinetic parameters of pseudo-second-order models for the adsorption of Pb(II) on the ZVI-MBC.

Pseudo-second-order			
q_e, exp (mg/g)	k_2 (g/mg min^{-1})	q_e, cal (mg/g)	R^2
48.65	0.0072	49.5049	0.9998

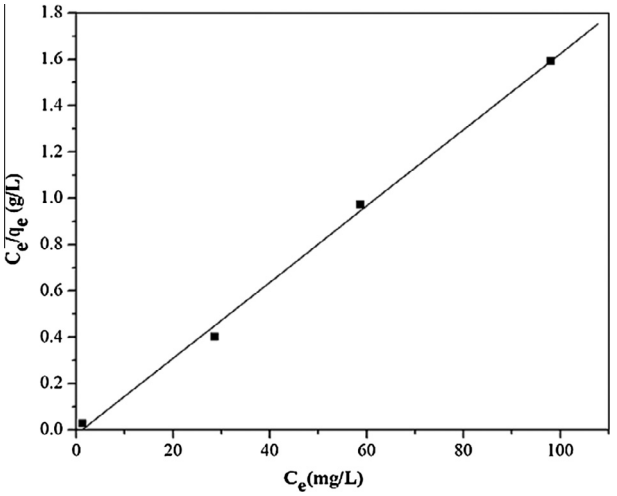

Figure 8 Linear plot of Langmuir isotherm of Pb(II) on ZVI-MBC.

Table 2 Langmuir and Freundlich isotherm constants.

Isotherm	Parameters
Langmuir	
q_m (mg/g)	60.80
b (L/mg)	0.8191
R^2	0.9947
Freundlich	
k_f (mg/g)	47.7089
n	9.1324
R^2	0.9910

The Freundlich isotherm can be applicable for modeling the adsorption of metal ions on heterogeneous surfaces and the linearized form of isotherm is expressed as

$$\log q_e = \log k_f + \frac{1}{n} \log C_e \tag{7}$$

where K_f (mg/g) and n are the Freundlich isotherm constants that represent the adsorption and the intensity of adsorbents. Fig. 9 shows the linear plot of Freundlich isotherm of Pb(II) adsorption on ZVI-MBC at 303 K. The fitted constants for the Freundlich isotherm model values of K_f, n and correlation coefficient (R^2) are calculated from the intercept and slope of the plot and are presented in Table 2. The values of $n > 1$ represent favorable adsorption condition [10,11] and the n value suggests that 9.1324 the ZVINPs is favorable for the adsorption of Pb(II) ions <!–Q9 replies = "Yes | No" type = "boolean": Please check the sentence "The values of n > 1. . .adsorption of Pb(II) ions" for clarity, and correct if necessary.-- > . Both the Langmuir and Freundlich isotherm models are fit well with the adsorption data

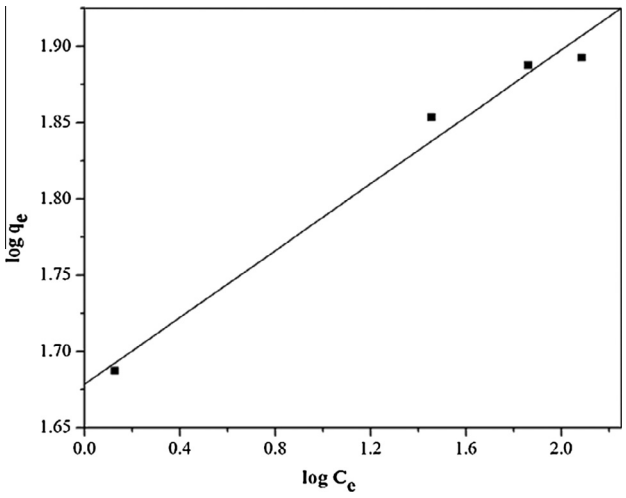

Figure 9 Linear plot of Freundlich isotherm of Pb(II) on ZVI-MBC.

Table 3 Adsorption capacities of different adsorbents for Pb (II) ions from aqueous solution.

Type of adsorbents	Capacity (mg/g)	Reference
Magnetic composite beads-chitosan	63.33	[20]
Magnetic hydrogels	126.40	[19]
Iron oxide coated sewage sludge	42.40	[23]
ZVI-MBC	60.8	This work

and have good correlation coefficients. The adsorption capacity of prepared ZVI-MBC for Pb(II) from Langmuir isotherm model compared with that of various adsorbents is given in Table 3.

4. Conclusions

In this study, we demonstrate the facile synthesis and characterization of zero valent iron magnetic biochar composites (ZVI-MBC). By using *E. globules* bark waste and honey we synthesized the ZVI-MBC by environmentally benign route. And this ZVI-MBC was successfully employed as adsorbent for removal of Pb(II) in aqueous solution. The results indicate that the equilibrium data fit well to Langmuir and Freundlich isotherm models. When the pseudo-second-order kinetic model was fit rather than the pseudo-first-order kinetic model, the maximum adsorption capacity was found to be 60.8 mg/g. Thus, the use of ZVI-MBC as an adsorbent will provide dual benefits.

References

[1] E. Agrafioti, D. Kalderis, E. Diamadopoulos, Arsenic and chromium removal from water using biochars derived from rice husk, organic solid wastes and sewage sludge, J. Environ. Manage. 133 (2014) 309–314.
[2] O.S. Amuda, A.A. Giwa, I.A. Bello, Removal of heavy metal from industrial wastewater using modified activated coconut shell carbon, Biochem. Eng. J. 36 (2007) 174–181.
[3] R. Azargohar, K.L. Jacobson, E.E. Powell, A.K. Dalai, J. Anal. Appl. Pyrolysis 104 (2013) 330–340.
[4] S.E. Bailey, T.J. Olin, R.M. Bricka, D.D. Adrian, A review of potentially low-cost sorbents for heavy metals, Water Res. 33 (1999) 2469–2479.
[5] B. Chen, Z. Chen, S. Lv, A novel magnetic biochar efficiently sorbs organic pollutants and phosphate, Bioresour. Technol. 102 (2011) 716–723.
[6] J.P. Chen, M. Lin, Equilibrium and kinetics of metal ion adsorption onto a commercial H-type granular activated carbon: experimental and modeling studies, Water Res. 35 (2001) 2385–2394.
[7] G. Crini, H.N. Peindy, F. Gimbert, C. Robert, Removal of C.I. basic green 4 (malachite green) from aqueous solutions by adsorption using cyclodextrin-based adsorbent: kinetic and equilibrium studies, Sep. Purif. Technol. 53 (2007) 97–110.
[8] P. Devi, A.K. Saroha, Risk analysis of pyrolyzed biochar made from paper mill effluent treatment plant sludge for bioavailability & eco-toxicity of heavy metals, Bioresour. Technol. 162 (2014) 308–315.
[9] P. Devi, A.K. Saroha, Synthesis of the magnetic biochar composites for use as an adsorbent for the removal of pentachlorophenol from the effluent, Bioresour. Technol. 169 (2014) 525–531.
[10] J. Gong, T. Liu, X. Wang, X. Hu, L. Zhang, Efficient removal of heavy metal ions from aqueous systems with the assembly of anisotropic layered double hydroxide nanocrystals@ carbon nanosphere, Environ. Sci. Technol. 45 (2011) 6181–6187.
[11] B.H. Hameed, D.K. Mahmoud, A.L. Ahmad, Equilibrium modeling and kinetic studies on the adsorption of basic dye by a low-cost adsorbent: coconut (*Cocos nucifera*) bunch waste, J. Hazard. Mater. 158 (2008) 65–67.
[12] Y.S. Ho, G. Mckay, Pseudo-second order model for sorption processes, Process Biochem. 34 (1999) 451–465.
[13] S. Lagergren, Zur theorie der sogenannten adsorption gelster stoffe, Kungliga Svenska Vetenskapsakademiens Seven Vetenskapsakad, Handlinger 24 (1898) 1–39.
[14] Z. Liu, F.S. Zhang, Removal of lead from water using biochars prepared from hydrothermal liquefaction of biomass, J. Hazard. Mater. 167 (2009) 933–939.
[15] V. Madhavi, T.N.V.K.V. Prasad, A.V.B. Reddy, B. Ravindra Reddy, G. Madhavi, Application of phytogenic zerovalent iron nanoparticles in the adsorption of hexavalent chromium, Spectrochim. Acta Part A Mol. Biomol. Spectrosc. 116 (2013) 17–25.
[16] J.O. Nriagu, J.M. Pacyna, Quantitative assessment of worldwide contamination of air, water and soils by trace metals, Nature 333 (1988) 134–139.
[17] D.H.K. Reddy, S.M. Lee, Magnetic biochar composite: facile synthesis, characterization, and application for heavy metal removal, Colloids Surf. A: Physicochem. Eng. Aspects 454 (2014) 96–103.
[18] V. Sarin, K.K. Pant, Removal of chromium from industrial waste by using eucalyptus bark, Bioresour. Technol. 97 (2006) 15–20.
[19] A. Selatnia, A. Boukazoula, N. Kechid, M.Z. Bakhti, A. Chergui, Y. Kerchich, Biosorption of lead (II) from aqueous solution by a bacterial dead Streptomyces rimosus biomass, Biochem. Eng. J. 19 (2004) 127–135.
[20] F. Shah, T.G. Kazi, H.I. Afridi, S. Khan, N.F. Kolachi, M.B. Arain, J.A. Baig, The influence of environmental exposure on lead concentrations in scalp hair of children in Pakistan, Ecotoxicol. Environ. Saf. 74 (2011) 727–732.
[21] W. Shao, L. Chen, L. Lü, F. Luo, Removal of lead (II) from aqueous solution by a new biosorption material by immobilizing Cyanex 272 in cornstalks, Desalination 265 (2011) 177–183.
[22] Y. Tao, L. Ye, J. Pan, Y. Wang, B. Tang, Removal of Pb (II) from aqueous solution on chitosan/TiO_2 hybrid film, J. Hazard. Mater. 30 (2009) 718–722.

[23] O.D. Uluozlu, A. Sari, M. Tuzen, M. Soylak, Biosorption of Pb(II) and Cr(III) from aqueous solution by lichen (*Parmelina tiliaceae*) biomass, Bioresour. Technol. 99 (2008) 2972–2980.
[24] S. Venkateswarlu, Y. SubbaRao, T. Balaji, B. Prathima, N.V.V. Jyothi, Biogenic synthesis of Fe_3O_4 magnetic nanoparticles using plantain peel extract, Mater. Lett. 100 (2013) 241–244.
[25] C.H. Weng, Modeling Pb(II) adsorption onto sandy loam soil, J. Colloid Interface Sci. 272 (2004) 262–270.
[26] WHO, WHO Guidelines for Drinking-Water Quality, fourth ed., WHO Press, Geneva, 2011, <http://www.who.int>.
[27] A. Yoshiaki, Y. Morio, S. Naoki, Y. Takeshi, Marker constituents of the natural antioxidant eucalyptus leaf extract for the evaluation of food additives, Biosci. Biotechnol. Biochem. 73 (2009) 1–6.
[28] Z.Y. Yao, J.H. Qi, L.H. Wang, Equilibrium, kinetic and thermodynamic studies on the biosorption of Cu(II) onto chestnut shell, J. Hazard. Mater. 174 (2010) 137–143.
[29] G. Zhang, J. Qu, H. Liu, A.T. Cooper, R. Wu, $CuFe_2O_4$/activated carbon composite: a novel magnetic adsorbent for the removal of acid orange II and catalytic regeneration, Chemosphere 68 (2007) 1058–1066.
[30] M. Zhang, B. Gao, S. Varnoosfaderani, A. Hebard, Y. Yao, M. Inyang, Preparation and characterization of a novel magnetic biochar for arsenic removal, Bioresour. Technol. 130 (2013) 457–462.